Enhanced dissipation of short gravity and gravity capillary waves due to parasitic capillaries

Xin Zhang

Citation: Physics of Fluids **14**, L81 (2002); doi: 10.1063/1.1519260
View online: http://dx.doi.org/10.1063/1.1519260
View Table of Contents: http://scitation.aip.org/content/aip/journal/pof2/14/11?ver=pdfcov
Published by the AIP Publishing

Enhanced dissipation of short gravity and gravity capillary waves due to parasitic capillaries

Xin Zhang
Scripps Institution of Oceanography, University of California, San Diego, La Jolla, California 92093-0213

(Received 30 April 2002; accepted 16 September 2002; published 7 October 2002)

The dissipation rate of short, mechanically generated, monochromatic surface waves was measured in order to determine the increased dissipation due to the generation of parasitic capillary waves. As the surface waves propagate freely, the decaying wave elevations were measured by an ultra-thin capacitance wire. Measurements indicate that the dissipation rate increases approximately with the square of the wave slope, AK, and the generation of parasitic capillaries depends on the wavelength of the surface waves. The maximum generation of parasitic capillaries coincides with a surface wave wavelength near 7 cm. Measured data fits a simple parameterized model of the dissipation rate reasonably well. © *2002 American Institute of Physics.* [DOI: 10.1063/1.1519260]

Viscous dissipation is generally negligible for gravity water surface waves. However, on the forward face of short gravity and gravity-capillary (SGGC) waves of a few centimeters to tens of centimeters in wavelength, there commonly resides a train of short capillaries. These capillaries are known as parasitic capillaries, and are carried forward quasi-steadily with the SGGC waves.[1,2] As the parasitic capillaries move forward with the SGGC waves, wave energy is transferred from these SGGC waves to the associated parasitic capillaries. This transfer of energy is through action of both the radiation stresses and surface pressure pulses at the crests of the SGGC waves. The energy of the capillary waves is then dissipated strongly by viscosity. Since the viscous dissipation is proportional to the inverse square of the wavelength, the energy loss associated with the capillaries can be many times that of the dissipation by the SGGC waves. In certain circumstances, this increased dissipation of SGGC waves due to parasitic capillaries cannot be ignored. Quantitative experimental results, however, have yet to be determined.

Interest in more accurate prediction of the parasitic-coupled short wave systems has arisen from applications such as microwave remote sensing of ocean surface and air–sea exchanges. In order to study such short wave systems, both wind-generated and mechanically generated waves have been observed. An advantage of mechanically generated wave experiments is that the observations can be directly compared with theories and numerical models. A brief, up-to-date review was given by Perlin and Schultz[3] together with an extensive list of references on this topic. The primary interest in observing short wind waves is to determine the wave spectrum (see Refs. 1, 4–7 for wind tank experiments and Refs. 8–10 for field measurements). It has been shown that, at the wavenumber, $k=O(10)$ rad/cm, the surface slope spectrum is peaked and the corresponding directional spreading narrowed.[6] This can be explained by the dominance of parasitic capillaries.[11] The spectrum of the short wind waves, in a range from 3 to 15 cm, are well below the Phillips' equilibrium spectral level even under conditions of a very long fetch of 90 m.[4,12] A possible inferential factor (among many others) causing this lower spectrum is the transfer of the wave energy to the parasitic capillaries. These effects, however, are not known quantitatively.

In order to perform experiments from which quantitative results could be obtained a proper apparatus was needed. With consideration of both water and wave qualities in mind we built a water tank with thick acrylic plates and supported it with a metal frame. The size of our tank is about 4 m long, 1 m wide, and 0.5 m high. It is wide enough to eliminate side wall effects, deep enough to hold the deep water wave assumption, and long enough to observe the waves at least a few wavelengths away from our mechanical wave maker. A wedge-type wave maker capable of generating a few Hz monochromatic waves was used at one end of the tank to generate waves with wavelengths from 5 to 15 cm. This long wave paddle, with a right-angle triangular cross section of height 10 cm and top width 4.5 cm, is made of foam filled fiberglass sheets. The paddle is strengthened by an aluminum bar running across the top. It is designed to be strong and light so that a stepper motor can drive the wave generating paddle system. Driving the system with a stepper motor allows precise control of the paddle motion, with programming flexibility. Two vertical hollow-shafts are attached near the ends of the wedge inhibiting its lateral movement. The wedge is coupled with the motor through gears and a driving belt. By micro-stepping the motor and properly adjusting the tension of the driving belt, the paddle can be moved up and down evenly and smoothly. Such even and smooth movement is necessary due to the inherent instability of steep gravity waves. Any unwanted motion disturbance can be amplified by the wave nonlinearity destabilizing the waveform quickly. To reduce wave reflection at the other end of the tank, we built a 1:10 sloping beach 1.5 m long. The roughened beach surface is made of 2-cm acrylic grid bound to an acrylic plate. The wave reflection from the beach is effectively reduced to less than 5%. To keep the water free from surface film and rust pollution, a surface skimmer-filter system is used and no metal parts come into contact with the

water. Using tap water in the tank, the surface skimmer-filter system was kept running at least 24 hours before the experiment. The surface tension was also monitored throughout the experiment by a tensiometer provided by NIMA Technology. These procedures keep the water surface effectively free from surface film during the experiments. Variance of surface tension changes the property of the capillary waves, and, thus, must be avoided.

Many different kinds of waves can be generated in the tank, but here we concentrate only on periodic waves with wavelengths between 5 and 15 cm. For the high slope wave cases, 1-D waves with slope, AK, up to 0.32 were continuously generated until lateral oscillations began to grow. Appearing a few minutes after the paddle starts, these oscillations resemble parametrically generated cross waves.[13,14] The developing oscillations are the standing waves resonant with the width of the tank, and their amplitude decays from the paddle. Prior to the appearance of these lateral oscillations, the paddle-generated waves were measured in a section 60 to 200 cm away from the wave paddle. It is reasonable to assume that the waves in this region are largely free from paddle forcing or flows induced by the paddle motion. We did not observe the development of the side-band instability[15] of the steep gravity waves. This can be attributed to our short working section and relatively slow growth rate of the amplitude modulation. There are also obliquely propagating, capillary-wave-like disturbances. They are generated at the sidewalls by the change of water–wall meniscus contact angles. The meniscus contact angle is changed from convex to concave at a point where the front face of the surface wave meets the wall, and this is where the disturbances are initiated. Keeping the sidewall wet, as suggested to us by Professor Longuet-Higgins, can mostly eliminate these disturbances.

In determining the properties of capillary waves, it is preferable to measure the surface slope directly rather than the wave height directly. The reasons are twofold. One is that the slopes of the parasitic capillaries can easily exceed the slopes of the underlying SGGC waves, making their slope very easy to measure. The other is that their amplitudes are much smaller than those of the carrier waves; any direct height measurement of the capillary waves would be highly difficult in the presence of the larger SGGC amplitudes. Accordingly, most past studies of parasitic and SGGC wave systems have made measurements with a surface slope gauge. Such gauges do, however, have limitations. The maximum slope that a surface slope gauge can measure often limits the steepest parasitic-coupled short wave system that can be investigated. The surface elevation can be found by integrating the slope measurement, which seems consistent with conventional capacitance wave gauge measurement[15] The direct measurement of the amplitudes of both capillary and gravity waves requires a very high measurement sensitivity and a very high signal to noise ratio.[16] For the purpose of determining the SGGC wave decay rate due to generating parasitic capillaries, we chose to use a simple capacitance wave gauge. The capacitance wire is made of a thin oxide coated tantalum wire of 0.1 mm in diameter.[17] The main concerns about using this gauge for this experiment were that it would create variations in meniscus and disturbances to the wavy surface. Such variation in meniscus may induce nonlinearities in transient response, which would limit the frequency response of a capacitance wire sensor. Fortunately, the meniscus effects induced by such a thin and uniform coated tantalum wire are relatively small[18] for measuring waves over a few centimeters. Moving our wire up and down at various frequencies also indicated that there were no surface disturbances other than the 2 mm circular meniscus area centered around the wire.

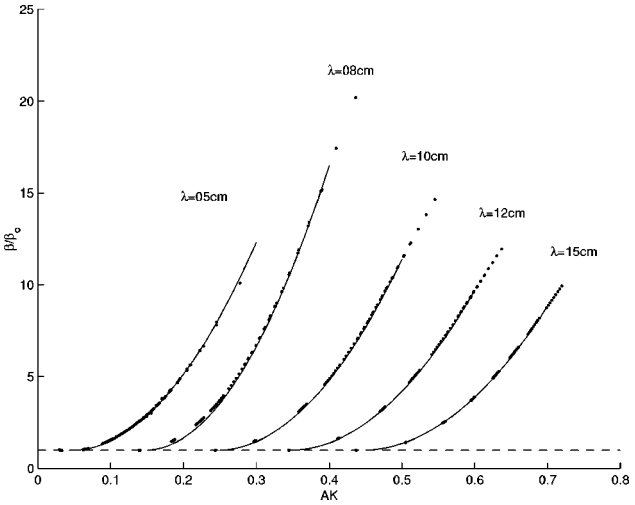

FIG. 1. Measured relative dissipation rate at different wavelengths. Dots are data points. Solid lines are the second order polynomial fits. Dashed line is the standard viscous dissipation, $\beta/\beta_o=1$. Each dissipation curve is offset horizontally by an increment value of 0.1. The dissipation rate increases nonlinearly with the increasing of the wave slope AK, and is of order 10 larger than the ideal waves without parasitic capillaries. The parasitic capillaries appear when the wave slope AK is somewhat in between 0.05 and 0.1 and, at the same time, the dissipation rate starts to depart from β_o.

In our experiments, we measured waves at various repeatable frequencies corresponding to wavelengths of 5, 8, 10, 12, and 15 cm, as estimated by the linear dispersion relation. Each run was recorded at a data-sampling rate of 256 Hz for 60 seconds prior to the development of any wave instability. The experiments lasted only one hour each, after which the water surface was cleaned by the skimmer-filter for at least 24 hours. Although it is understood that for nonlinear gravity waves, kinetic and potential energies are slightly different, we chose, due to the difficulty involved in obtaining kinetic energy data, to approximate the dissipation rate of wave energy using solely the potential energy. The wave elevations along the center of the tank were measured sequentially at multiple wavelengths apart to minimize the potential error due to weak wave reflections from the beach. Changes in wave potential energy were calculated by integrating the surface time series and comparing this result with the adjacent measurements. Our analysis indicates that the dissipation rate increases nonlinearly with the increasing of the slope AK, and is of an order of 10 times larger than ideal waves without parasitic capillaries (Fig. 1). The parasitic capillaries appear when the wave slope AK is between 0.05 and 0.1 depending on the SGGC wave length. Also, between these same wave slopes, the dissipation rate, β (energy $E=E_o e^{-\beta t}$), departs from and is greater than the standard

viscous dissipation, $\beta_o = 4\nu K^2$ ($E = E_o e^{-\beta_o t}$). Here, ν is the kinematic viscosity, and K is the SGGC wave wavenumber.

The dynamics of parasitic capillaries can explain this increased dissipation. The parasitic capillaries propagate at a zero or very slow phase speed relative to the underlying SGGC wave crests. Much of capillary wave energy should be dissipated by viscosity quickly. For example, for a capillary wave with a wavenumber, $k = 10$ rad/cm, the wave energy at one second is $e^{-4\nu k^2} < 2\%$. Thus, more than 98% of its energy is dissipated in 1 second. Without a constant supply of energy, the parasitic capillaries would be wiped out in less than one second by viscosity. For the capillaries to continue to be present, energy must come from the SGGC waves. The SGGC wave energy is transferred to the parasitic capillaries in two ways. Near a SGGC wave crest, a narrow pressure pulse of surface tension associated with the high local curvature[2,19] generates parasitic capillaries. These capillaries have an amplitude proportional to the pressure, that decays quickly with e^{-bk}, where b is the breadth of the local pressure of a sharp crest. Also, in a coordinate moving with SGGC waves, parasitic capillaries propagate against the orbital velocity, q, downward from the crest and onto the forward face of the underlying SGGC waves. Thus, the energy flux lost to the capillaries is equal to the work done by the orbital velocity acting against the radiation stress of the capillaries:

$$\frac{\partial}{\partial s}[E_c(q + c_g)] + S\frac{\partial q}{\partial s} + 4\nu k^2 E_c = 0, \tag{1}$$

where E_c is capillary wave energy, c_g the group velocity, S the radiation stress and s the local arc length of the underling SGGC waves. In general, both the surface tension pressure pulse and orbital compression increase with increasing wave slope AK, resulting in a greater energy flux into the capillaries. Viscosity or capillary rollers then effectively dissipate this capillary wave energy[21] transferred from the SGGC wave. For SGGC waves with a wavelength shorter than about 7 cm,[19] the parasitic capillaries pass through the SGGC wave troughs and are stretched, transferring energy to the backward face of the adjacent SGGC wave. In these cases, one might expect a decrease in the energy gained by capillaries, and, thus, an overall decrease in dissipation of the SGGC waves.

Since parasitic capillaries had moderate slopes within our experimental range ($<35°$), their viscous dissipation rate was well approximated by linear dissipation. The dissipation due to viscosity can be directly estimated by integrating capillary wave slope profiles over a SGGC wave period:

$$-\frac{\partial E_g}{E_g \partial t} = 4\nu K^2 - \frac{1}{2\pi E_g}\int \frac{\partial E_c}{\partial t} d\varphi$$

$$= 4\nu K^2 + \frac{1}{2\pi E_g}\int 4\nu k^2 E_c d\varphi, \tag{2}$$

where E_g and E_c are wave energy of SGGC and capillaries, K and k the wave number of SGGC and capillary waves. The capillary energy is proportional to the square of wave slopes, θ, thus

TABLE I. Parasitic capillary dissipation estimated from surface slope profiles.

Wave length	AK	β/β_o	Reference
8 cm	0.30	45	theory (Ref. 20)
8 cm	0.28	8.0	theory (Ref. 20)
8 cm	0.26	1.9	theory (Ref. 20)
8 cm	0.24	1.1	theory (Ref. 20)
9.1 cm	0.26	1.7	experiment (Ref. 15)
7.3 cm	0.265	3.5	experiment (Ref. 22)
5.2 cm	0.20	2.7	experiment (Ref. 22)

$$-\frac{\partial E_g}{E_g \partial t} = 4\nu K^2\left(1 + \frac{\overline{k^2\theta^2}}{(AK)^2}\frac{T}{g}\right), \tag{3}$$

where $\overline{k^2\theta^2} = 1/2\pi \int k^2\theta^2 d\varphi$. Although our wave wire data were not sufficient to resolve the capillary wave slopes, we were able to estimate dissipation from a number of published slope profiles, including both theoretical and experimental profiles. The dissipation estimates are listed in Table I. Our measured dissipation of the SGGC waves was greater than the estimated dissipation from experimental data, but was less than that from theoretical data. For a conclusive estimation of capillary dissipation, a larger number of measured surface slope profiles are needed.

The parasitic capillary wave slopes are dependent on the long wave parameters, such as long wave crest curvature, orbital velocity and phase. Unfortunately, these parameters are difficult to measure practically. However, from our measurements of the energy dissipation, it is possible to approximate the dissipation, $\partial E/\partial t$, as a function of the long wave slope, AK. We can fit the experimental data very well with a simple second order polynomial:

$$\beta/\beta_o = 1 + \alpha(AK - S_o) + \gamma(AK - S_o)^2 \quad \text{for} \quad AK > S_o, \tag{4}$$

where α, γ and S_o are the fitting parameters. S_o is the threshold slope, AK, when parasitic waves start to appear. α is very close to 1 and changes little regardless of wavelength. γ varies with wavenumber as given in Table II. The last term on the right side of Eq. (4) is the dominant factor in the ratio of enhanced capillary dissipation to viscous dissipation. It reflects the efficiency among SGGC waves of different wavelengths in generating parasitic capillaries. With $S_o = 0.05$, $\alpha \equiv 1$, and $\gamma(K)$ as specified by linear fittings, the calculated dissipation rate, β, for different wavelengths is shown in Fig. 2, along with the measured data. Although this parameterization is not sophisticated, it matches the measurements reasonably well. In applications such as wind wave spectrum, the first two terms are an order magnitude smaller than the third nonlinear term, and the dissipation can further be simplified as

TABLE II. The parameter γ as a function of K.

K (rad/cm)	1.26	0.79	0.63	0.52	0.42
γ	184	249	166	139	126

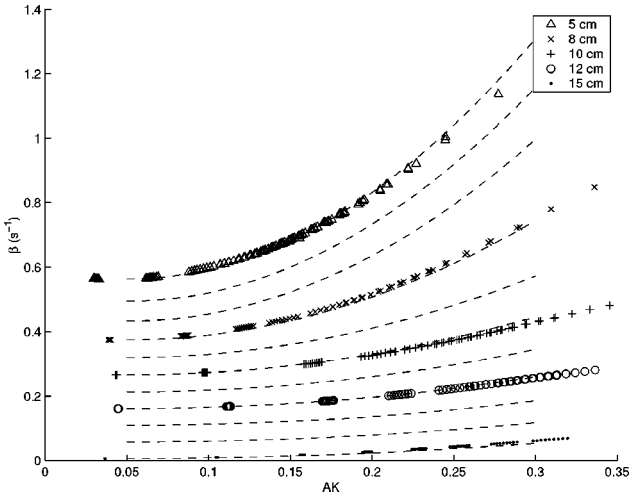

FIG. 2. Comparison between the empirical model and experimental data. The lines are the dissipation rate calculated from the model for wavelength 5 to 15 cm at an 1 cm increment, and symbols are measured data. Each dissipation curve is offset upward by an increment value of 0.05.

$$D = \frac{\partial E}{\partial t} \approx -4\nu K^2 \gamma (AK - S_o)^2 E$$

$$\propto -\gamma(K)(g + TK^2)^{-1} K^4 E^2. \tag{5}$$

ACKNOWLEDGMENT

This work was supported by the National Science Foundation uner Grant No. 9811262.

[1]C. S. Cox, ''Measurement of slopes of high-frequency wind waves,'' J. Mar. Res. **16**, 199 (1958).
[2]M. S. Longuet-Higgins, ''The generation of capillary waves by steep gravity waves,'' J. Fluid Mech. **16**, 138 (1963).
[3]M. Perlin and W. W. Schultz, ''Capillary effects on surface waves,'' Annu. Rev. Fluid Mech. **32**, 241 (2000).
[4]B. Jähne and R. S. Riemer, ''Two-dimensional wave number spectra of small-scale water surface waves,'' J. Geophys. Res., [Oceans] **95**, 11531 (1990).
[5]P. A. Hwang, D. B. Trizna, and J. Wu, ''Spatial measurements of short wind waves using a scanning slope sensor,'' Dyn. Atmos. Oceans **20**, 1 (1993).
[6]X. Zhang, ''Wavenumber spectrum of very short wind waves: An application of 2-D Slepian windows to the spectral estimation,'' J. Atmos. Ocean. Technol. **11**, 489 (1994).
[7]T. Hara, E. Bock, and M. Donelan, ''Frequency-wavenumber spectrum of wind-generated gravity-capillary waves,'' J. Geophys. Res., [Oceans] **102**, 1061 (1997).
[8]P. A. Hwang, S. Atakturk, M. A. Sletten, and D. B. Trizna, ''A study of the wavenumber spectra of short water waves in the ocean,'' J. Phys. Oceanogr. **26**, 1266 (1996).
[9]T. Hara, E. J. Bock, J. Edson, and W. McGillis, ''Observation of short wind waves in coastal waters,'' J. Phys. Oceanogr. **28**, 1425 (1998).
[10]X. Zhang, ''Observations on waveforms of capillary and gravity-capillary waves,'' Eur. J. Mech. B/Fluids **18**, 373 (1999).
[11]X. Zhang, ''Capillary-gravity and capillary waves generated in a wind wave tank: Observations and theories,'' J. Fluid Mech. **289**, 51 (1995).
[12]O. M. Phillips, ''Spectral and statistical properties of the equilibrium range in wind-generated gravity waves,'' J. Fluid Mech. **156**, 505 (1985).
[13]A. F. Jones, ''The generation of cross-waves in a long deep channel by parametric resonance,'' J. Fluid Mech. **138**, 53 (1984).
[14]J. W. Miles and D. M. Henderson, ''Parametrically forced surface waves,'' Annu. Rev. Fluid Mech. **22**, 143 (1990).
[15]T. B. Benjamin and J. E. Feir, ''The disintegration of wave train on deep water,'' J. Fluid Mech. **27**, 417 (1967).
[16]J. H. Chang, R. N. Wagner, and H. C. Yuen, ''Measurement of high frequency capillary waves on steep gravity waves,'' J. Fluid Mech. **86**, 401 (1978).
[17]M. Perlin, H.-J. Lin, and C-L. Ting, ''On parasitic capillary waves generated by steep gravity waves: An experimental investigation with spatial and temporal measurements,'' J. Fluid Mech. **255**, 597 (1993).
[18]R. D. Chapman and F. M. Monaldo, ''A novel wave height sensor,'' J. Atmos. Ocean. Technol. **12**, 190 (1995).
[19]C. A. Keller and R. D. Chapman, ''A laboratory investigation of the dynamic response of capacitive wave gauges,'' JHU/APL Report STD-R-350, 1980, 56 pp.
[20]M. S. Longuet-Higgins, ''Parasitic capillary waves: A direct calculation,'' J. Fluid Mech. **301**, 79 (1995).
[21]M. S. Longuet-Higgins, ''Capillary rollers and bores,'' J. Fluid Mech. **240**, 659 (1992).
[22]A. V. Fedorov, W. K. Melville, and A. Rozenberg, ''An experimental and numerical study of parasitic capillary waves,'' Phys. Fluids **10**, 1315 (1998).